Physical Model Analysis of Foam–TCE Displacement in Porous Media

Seung-Woo Jeong
Korea Environment Institute, Bulgwang-Dong, Seoul, 122-706, Korea

M. Yavuz Corapcioglu
Environmental and Water Resources Engineering Div., Dept. of Civil Engineering, Texas A&M University, College Station, TX 77843

A glass micromodel was experimented to study the coupled effects of the apparent viscosity and mobility of surfactant foam (SF) on the displacement of residual trichloroethylene (TCE) during SF flooding. The SF floods operated under moderate interfacial tension (4.9 dyne/cm) of surfactant solution with TCE and pressure gradient (20 − 200 kPa) conditions showed relatively different foam behaviors to the higher pressure gradient conditions. The apparent viscosity of SF seems to be less affected by changes in surfactant concentration and affected more by the gas fraction in SF or the bubble size of SF. As the total SF flow rate and the gas injection velocity increased, the apparent SF viscosity decreased and the SF mobility increased. The latter characteristic led to an increase in the TCE displacement efficiency although SF under low-pressure gradients resulted in flow channeling. The experiment results imply that the SF flood for environment application would be affected by operating conditions and distribution of residual contaminants.

Introduction

Recently, the use of surfactant foam has been suggested for environmental remediation (Hirasaki et al., 1997a,b; Chu et al., 1996; Rothmel et al., 1998). The operating conditions of these foam-flooding investigations with respect to applied interfacial tension (IFT) systems and foam-generation methods were similar to those of foam flooding used for enhanced oil recovery (EOR). A surfactant-foam (SF) study employing a moderate IFT (4.9 dyne/cm) and pressure gradient system (20–200 kPa/m) demonstrated the removal of residual trichloroethylene (TCE) trapped in a porous medium (Jeong et al., 2000). The use of SF with a moderate IFT with TCE reduced the vertical migration tendency of TCE, which has been of concern in the remediation of groundwater aquifers contaminated by TCE spills. However, only a little information about foam behaviors has been provided in the environmental literature.

Foam generation and bubble size affect the foam flow behavior through porous media (Ettinger and Radke, 1992). Foam is usually generated either by an external foam generator or by an internal foam-generation method. Both foam-generation methods use pressure gradients greater than 650 kPa/m and generate very thin liquid films between bubbles (Hudgins and Chung, 1990; Llave et al., 1990; Minssiex, 1974), that is, this study calls the pressure gradients as high pressure gradients. The SF used in this study was generated by the simultaneous injection of surfactant solution and air through an injection tube so bubbles formed between the liquids slug. The thickness of SF lamellae (such as the liquid wall between bubbles) in an injection tube of 1.5-mm diameter was about 3.5 mm. The generated pressure gradient by SF flooding used in this study ranged from 20 to 200 kPa/m. These different physical properties of foams might affect their propagation in porous media. Although the physical properties of foam generated under high-pressure gradients, such as the apparent viscosity and mobility, have been well understood, no study of the apparent viscosity and mobility of foam generated at relatively low-pressure gradients has been conducted.

The objectives of this study were to understand SF behavior flowing under moderate IFT and relatively low-pressure gradients in terms of the apparent viscosity and mobility of SF, and to determine the most important factor affecting the SF behavior in order to enhance the TCE displacement. This study refers to foam as general foams, while the term SF refers to the surfactant foam used in this study.

Correspondence concerning this article should be addressed to S.-W. Jeong.

Background

The use of foam in the petroleum industry originated from gas mobility control for gas flooding. By using gas injection (CO_2, hydrocarbon gases, and so on), all EOR techniques have experienced poor sweep efficiency because of gas channeling and gravity override in a porous media (Kuhlman, 1990; Schramm et al., 1990). These two major problems occurred because of the higher mobility of the gas phase than that of the oil phase. However, the gas phase injected as a foam exhibited a higher gas viscosity of up to 1,000 times that of the original constituent (Huh et al., 1989; Manlowe and Radke, 1990; Rossen et al., 1991). The mobility of gas was strongly correlated to the apparent viscosity of gas. The concepts of foam mobility or the gas mobility in a porous media are a matter of controversy in the petroleum literature and two different foam behaviors have been reported when the gas velocity increased. While Huh et al. (1989) reported that the shear-thickening behavior of foam was observed in micromodel experiments, most of the other studies observed the shear-thinning of foam (Chang et al., 1990; Falls et al., 1989; Lee et al., 1990; Owete and Brigham, 1987). Most studies on the apparent viscosity and mobility of foam were performed without residual oil in a porous media. No effort has been made to establish a correlation between the physical properties (such as apparent viscosity and mobility) of foam and dense nonaqueous phase liquid (DNAPL) displacement efficiency.

Only a few studies of environmental remediation have dealt with foams. Hirasaki et al. (1997a,b) performed foam-flooding experiments for DNAPL removal in the laboratory and then made the first field demonstration. They recovered 99% of the residual TCE in a sand pack by foam flooding, and achieved an 87.5% removal of a DNAPL mixture from a contaminated site. They used an anionic surfactant solution with 1,500 ppm NaCl. This type of surfactant solution will result in the middle phase micro-emulsion conditions (Hirasaki et al., 1997a; West and Harwell, 1992). Chu et al. (1996) performed surfactant foam-flooding studies for residual dodecane removal. Rothmel et al. (1998) evaluated a surfactant foam technology involving bioremediation, and achieved 75% removal of residual TCE by foam alone. Recently, Chowdiah et al. (1998) reported some physical information about the pressure gradients and apparent viscosity when foam was applied for soil remediation. They applied high-pressure gradients during foam flooding, but the use of ethanol reduced the pressure gradient down to 45 kPa/m. They also suggested a potential application of diverting foam flow to a low permeability zone. They noted that foam with similar mobilities can be achieved even if the permeabilities of the porous medium are different, and mentioned the possibility of preventing flow channeling by foam flooding.

Experimental and Calculation Methods

Experimental setup

The micromodels were made of glass and etched by photochemical methods to fabricate solid grains and pores (Buckley, 1991). A micromodel with homogeneous properties, as shown in Figure 1, was used in this study. The network in the micromodel consisted of mutually perpendicular channels (or throats) with diamond-shaped pores and smaller nodes alternating at the interactions of throats. The permeability and porosity of the micromodel were measured as 1.7×10^{-7} cm^2 and 0.27, respectively. Detailed procedures to determine the micromodel properties and a schematic of the experimental apparatus have been described in Jeong et al. (2000).

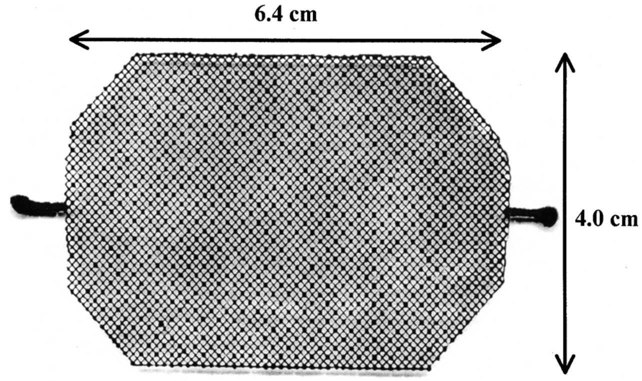

Figure 1. Homogeneous glass micromodel.

Simultaneous injection of surfactant solution and air produced SF in the injection tube (2 mm OD × 1.5 mm ID; Waters Corp.) of the micromodel. A pressure transmitter (Model 600, AutoTran Inc.) monitored the pressure variation of the injected SF every 30 s. During the injection of 25 pore volumes (PV) SF into the micromodel, the results monitored were stored in a computer containing a data-logging software (QuickLog, Strawberry Tree Inc.) and then used for the apparent viscosity and mobility calculations.

Measurement of the apparent SF viscosity

The apparent viscosity is the viscosity determined for a non−Newtonian fluid without reference to a particular shear rate. The apparent viscosity is usually determined by a method applicable to Newtonian fluids (Falls et al., 1989; Lee et al., 1990). Thus, Darcy's law is used to determine the apparent viscosity of a fluid

$$\mu_a^{\text{meas.}} = \frac{k_o k_r \nabla P}{q_T} \tag{1}$$

where $\mu_a^{\text{meas.}}$ is the measured apparent viscosity, q_T is the Darcy velocity, k_o is the intrinsic permeability of the porous medium, k_r is the relative permeability, and ∇P is the pressure gradient along a horizontal porous medium.

The gas-phase pressure was continuously monitored during all experiments. An average gas-phase pressure was determined from the pressure data obtained during 20−25 PV flooding, which was assumed to be the steady state. At steady state, q_T would be constant and equal to the injection flow rate per unit area, since the aqueous phase saturation during the foam flooding would be constant within the porous medium (Ettinger and Radke, 1992; Persoff et al., 1991). The injection flow rate was the summation of injection flow rates of the surfactant solution and the gas phase (air). The flow rate of the gas phase was corrected with pressure and temperature. The relative permeability was calculated by Corey's equation using the sum of the liquid and gas-phase saturation after SF flooding.

Three concentrations of surfactant solution, that is, 0.5, 1, 2% (weight basis), were evaluated to examine the effect of surfactant concentration on the apparent SF viscosity. An anionic surfactant of sodium $C_{14\text{-}16}$ olefin sulfonate (Bio-terge AS-40, Stepen Co.) was used in the experiments. To determine the effect of gas fraction (GF) on the apparent viscosity, two GFs of 66% and 85% were applied. GF is defined as the ratio of the gas volume to SF volume.

The micromodel was cleaned once by 0.05 N sulfuric acid including potassium chromate, followed by methanol after each experiment. TCE (Fischer Scientific Inc.) was dyed with Oil-Red-O (Aldrich Inc.), specifically, 0.5 g/L. Dyed TCE was injected by a syringe into a micromodel saturated with deionized, distilled water until the breakthrough was reached. The micromodel saturated with dyed TCE was then flushed by water at the rate of 0.45 mL/h. After this water flooding, the mean residual TCE saturation of the micromodel was measured as 0.32 by visualization and quantification (Jeong et al., 2000). SF was then applied to the micromodel, and the inlet gas pressure was continuously monitored. SF flooding experiments in a control micromodel without any residual TCE containing water only were also performed for comparison. Although the pressure responses in the micromodel with residual TCE were somewhat higher than those without TCE at the early stages of the experiment, the pressure variations at steady state were relatively similar to each other.

Calculated apparent SF viscosity

Hirasaki and Lawson (1985) developed a theoretical expression for apparent foam viscosity in a smooth capillary. In addition, a theoretical model was developed to account for the pore constriction in homogeneous bead packs placed in glass tubes (Falls et al., 1989). Four components contribute to the apparent viscosity: (1) the liquid viscosity of the slugs of surfactant solution between the bubbles, μ_{com1}, (2) the resistance between bubbles and channel walls during the foam flow, μ_{com2}; (3) the surface-tension gradient due to the surfactant concentration gradient, μ_{com3}; (4) the resistance due to pore constrictions, μ_{com4}. Each component is expressed by

$$\frac{\mu_{com1}}{\mu_w} = L_s n_L \tag{2}$$

$$\frac{\mu_{com2}}{\mu_w} = \left[\frac{0.85 n_L r_{cap}}{r_c/r_{cap}}\right]\left(3\mu_w v_g/\sigma\right)^{-1/3}\left[1+\left(r_c/r_{cap}\right)^2\right] \tag{3}$$

$$\frac{\mu_{com3}}{\mu_w} = n_L r_{cap}\left(3\mu_w v_g\right)^{-1/3}\sqrt{N_S}\tanh\left(\frac{L_{BD}}{2}\right) \tag{4}$$

$$\frac{\mu_{com4}}{\mu_w} = \xi_1 n_L r_{cap}\left(\frac{3\mu_w v_g}{\sigma}\right)^{-1} \tag{5}$$

The nomenclature used in theses expressions and the values used for the apparent SF viscosity calculations are given in Table 1. We modified the parameters of the theoretical expression given by Falls et al. (1989) for bead packs for the micromodel used in this study, as explained in the footnotes to Table 1. The calculated apparent SF viscosity of each component was determined to describe how each component affects the total apparent viscosity calculations.

Table 1. Theoretical Apparent Viscosity Expressions (Eqs. 2–5) and Values Used in Calculations (GF = 66%)

Definition	Value for Micromodel Exp.
L_s = length of liquid slugs between the bubbles,* cm	0.35
n_L = number of lamellae per unit length,** lamellae/cm	1.2
r_{cap} = capillary radius, cm, $\phi d_b/[3(1-\phi)+2d_b/d_t]$	0.000957
r_c = radius of curvature of plateau border in a foam lamella, cm $\{(1-\Gamma)/[3(1-\pi/4)\Gamma](r_B/r_{cap})^3\}^{1/2} r_{cap}$	1.28
Γ = foam quality†	0.66
r_B = foam bubble radius,†† cm	0.12
μ_w = viscosity of aqueous phase, cP	1.029
σ = surface tension, dyne/cm	33.34
N_s = dimensionless group, β/r_c, cm, β (= 5cm, parameter in the smooth-tube viscosity model)	3.92
L_{BD} = dimensionless bubble length, cm, $(L_B/r_c)(3\mu_w v_g/\sigma)^{-1/3}/\sqrt{(N_s)}$	Changed by v_g
v_g = gas velocity, cm/s	Varied
ϕ = porosity	0.27
d_b = bead diameter,‡ cm	0.008
d_t = tube diameter,‡‡ cm	0.257
ξ_1 = geometrical factor	0.56

*Average length of a liquid slug in SF was calculated based on directly measured individual lengths in the injection tube.
**Average number of liquid slugs in SF.
†Equal to gas fraction value.
††Average bubble radius in the SF train that was flowing in the injection tube.
‡Average diameter of solid grains.
‡‡The diameter of the equivalent circular tube calculated from the rectangular cross-sectional area of the micromodel.

The mobility of SF in porous media during the SF flooding

The mobility of SF, λ_{SF}, is defined by Eq. 6 (Lee and Heller, 1988; Lee et al., 1990)

$$\lambda_{SF} = \frac{q_T}{\nabla P} \tag{6}$$

The mobility is inversely proportional to the apparent viscosity, as given by Eq. 1. The pressure drop was monitored as described earlier and used to calculate the mobility of SF. The mobility was expressed in terms of cm^2/cP.

Capillary number

The capillary number is a dimensionless number representing the ratio between the viscous and capillary forces

$$N_{Ca} = \frac{\mu_a q_T}{\sigma\cos\theta} = \frac{k_o k_r \nabla P}{\sigma\cos\theta} \tag{7}$$

where μ_a is the apparent viscosity, σ is the IFT between the displacing and displaced fluids, and θ is the contact angle with the solid. The relative permeability, k_r, was calculated by Corey's equation (Corey, 1986). Interfacial tensions of 0.5, 1, and 2% surfactant solution with red-dyed TCE were 6.4

dyne/cm, 5.7 dyne/cm, and 4.9 dyne/cm, respectively. The measured contact angle between the dyed TCE on the glass and the surfactant solutions was 130 degrees.

Results and Discussion

Effect of gas fraction and surfactant concentration on apparent SF viscosity

Figure 2a shows pressure gradients as a function of total flow rate (sum of surfactant and air velocity). The pressure gradients were the base values for determining the apparent viscosity and mobility of SF. Figure 2b shows the effect of GF and surfactant concentration on the apparent viscosity of SF. Two GFs (66 and 85% GF) and three different surfactant concentrations (0.5, 1, and 2%) were evaluated as a function of the injection rate, q_T. As the injection velocity increased, the apparent viscosity of SF decreased at both 66% GF and 85% GF. The results are consistent with those of a previous study (Falls et al., 1989). While the effect of GF was shown to be distinguishable, little difference in the apparent viscosity with surfactant concentration change was observed at 66% GF.

This study attributed the difference in apparent viscosity at different GFs to the effect of foam bubble size or foam texture. Since more air was injected to produce an SF at 85% GF, the bubble size of SF produced would be larger than that of the SF at 66% GF. Foam with smaller bubble sizes yielded higher apparent viscosity during its flow through porous media, because the viscous resistance between the foam bubbles and capillary wall depended on the bubble density (Hirasaki and Lawson, 1985). In this study, the bubble density is defined as the number of lamellae per unit length of the injection tube. Foam that used EOR consists of many bubbles and thin liquid films between the bubbles, yielding a high bubble density, whereas the SF at 66% GF consists of 1.2 bubbles per 1 cm length of the injection tube, and has thick lamellae. Although the apparent viscosity of foam ranged around 10^3 cP at the injection velocity of 100 cm^3/cm^2-h (Falls et al., 1989), the apparent viscosity of SF at the same velocity was about 20 cP. Foam with the higher bubble density exhibited higher apparent viscosity due to the high resistance resulting from more lamellaes. Therefore, the effect of SF texture on the apparent viscosity was also observed, even at such low bubble densities, that is, 1.2/cm at 66% GF and 0.6/cm at 85% GF, as shown in Figure 2b. The SF at 66% GF, which has smaller bubble sizes, produced a higher apparent viscosity than 85% GF.

The small difference in the apparent SF viscosity by surfactant concentration change can be of interest. Some researchers reported that the apparent viscosity and mobility of the foam were significantly affected by surfactant concentration (Heller, 1994; Lee and Heller, 1988). It was expected that one significant difference between the two results arose from the foam rupture and regeneration. As mentioned earlier, SF was injected under low-pressure gradients and had low bubble density, whereas most other foams were generated or operated under high-pressure gradients and had a higher bubble density than the bubble density of SF. Micromodel visualization confirmed this expectation and also revealed the importance of foam texture in foam flow. Injected SF was first entrapped in larger pores. The observed bubble sizes were uniform and large throughout the entire SF flooding, indicating a low foam density. Bubbles of SF were seldom ruptured due to their thick lamellae, which appeared to be independent of surfactant concentration. Foam under high-pressure gradients would undergo foam rupture and regeneration as it flowed through a porous media (Kovscek et al., 1994; Owete and Brigham, 1987; Ransohoff and Radke, 1988). The occurrence of these two phenomena (rupture and regeneration) increased with increasing surfactant concentration and pore aspect ratio (pore throat size/pore body size) in foam flooding (the same references with the previous one). The frequent variation of bubble density during foam flooding greatly affects the apparent viscosity and mobility of foam. Based on the results in this study, the apparent viscosity of SF seems to be less affected by changes in surfactant concentration and affected more by the air injection velocity.

Components of the apparent viscosity

Four components contribute to the apparent viscosity, as mentioned in the subsection on calculated apparent SF vis-

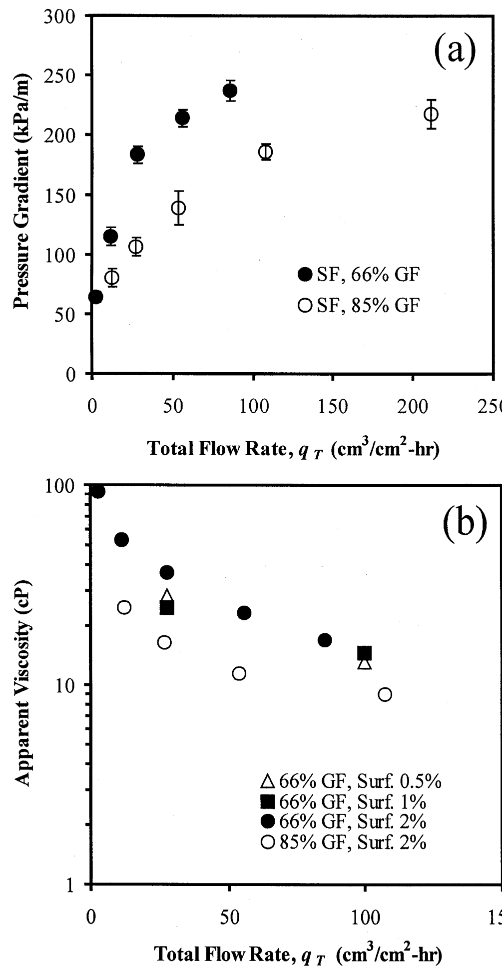

Figure 2. (a) Pressure gradients during SF floods; (b) effect of the total SF flow rate on apparent SF viscosity: two GF, 66 and 85%; three surfactant concentrations, 0.5, 1, and 2% sodium olefin sulfonate(w) by weight basis.

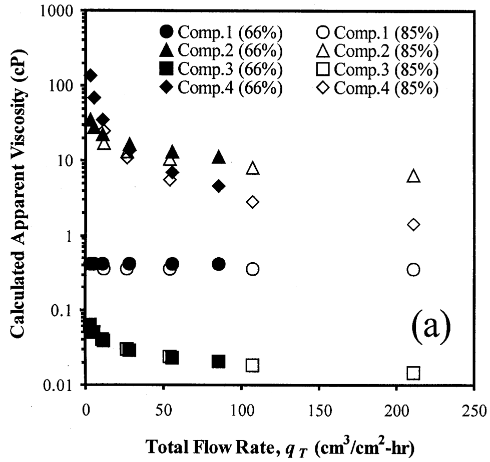

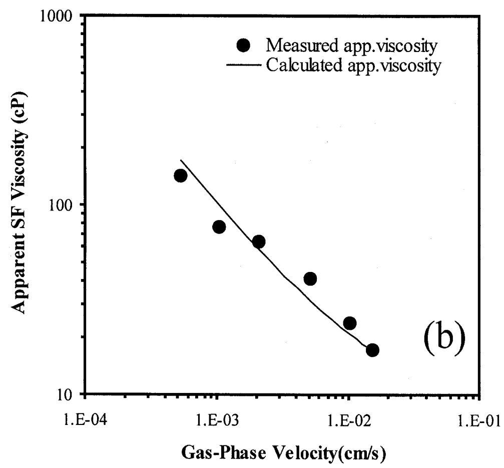

Figure 3. (a) Contribution of each component to total apparent viscosity of SF for GFs at 66% and 85%.

The apparent viscosity was calculated theoretically by Eqs. 2 to 5. (b) Comparison of the calculated apparent viscosity with measured apparent viscosity (conditions: 66% GF, 2%(w) surfactant).

cosity. This study calculated the theoretical apparent viscosity of SF in the homogeneous micromodel, and then compared it with the measured apparent viscosity to find the major contributing components to the apparent viscosity. Figure 3a shows the variations in apparent viscosity due to each component as a function of the SF flow rate.

Predictions of the theoretical apparent viscosity, which was the summation of each component, were compared with measured results, as shown in Figure 3b. The apparent SF viscosity estimated by the theoretical expression was consistent with the measured apparent SF viscosity. Therefore, the theoretical expression for predicting the apparent viscosity of foam can be used to determine the contribution of each component. Two components, the resistance between the bubbles and channel walls, μ_{com2}, and the resistance due to pore constrictions, μ_{com4}, were the dominant contributors to the total apparent SF viscosity. The other components were negligible compared to the two components. Based on the results presented in the previous section and the contribution results here, we can conclude that the apparent viscosity of SF is influenced by the bubble size of SF, the total flow rate, and the air injection velocity.

Role of apparent viscosity on TCE displacement

Ultimately, it is important to know whether there is a correlation between the apparent viscosity of SF and TCE removal. The TCE displacement efficiency by SF flooding was found to be inversely correlated with the apparent viscosity, as shown in Figure 4a, that is, results of SF floods at 66% GF and 2% surfactant solution. Figure 4b and 4c illustrate the same TCE displacement efficiency and gas saturation as Figure 4a, in terms of three different properties: the apparent viscosity (measured), the total flow rate, and the capillary number. The TCE displacement efficiency was obtained by the ratio of the reduced TCE saturation after 25 PV injection to the initial TCE saturation. A solubilized portion was excluded from the reduced TCE saturation based on the results of surfactant floods. The gas saturation was determined by measuring the gas-phase areas.

A higher TCE removal efficiency was obtained at both lower apparent viscosity and higher flow rate. Displacement of trapped organics in porous media would be strongly affected by the capillary number (Stegemeier, 1977). Figure 4c shows the higher capillary number resulted in the higher TCE removal efficiency. The capillary number is proportional to the product of the apparent viscosity and the flow rate as shown in Eq. 7. Displacement of 10% of residual TCE can be obtained with decreasing apparent viscosity by 20 cp and increasing q_T by 45 cm/h. This relation indicates that the total flow rate contributes more to the determination of the capillary number than the apparent viscosity with Eq. 7.

One other contribution of the apparent viscosity to foam flow is the mobility of foam in porous media. The mobility of a fluid in porous media is strongly affected by the apparent viscosity and might then affect the TCE displacement efficiency to a large extent. Details are discussed in the next subsection.

Mobility of SF in porous media and TCE displacement

Figure 5 shows the effect of the total flow rate of SF on the mobility and apparent viscosity of SF. The results of the mobility and the apparent viscosity data were contrary to each other. While the apparent viscosity decreased with increasing injection velocity, the mobility of SF increased with increasing velocity. The data exhibit a shear-thinning behavior of SF. As noted in the Introduction section, the foam mobility has been a controversial topic in the literature.

Reduced gas mobility using foam not only can reduce gas channeling in flooding, but also can produce a stable displacement front. In a stable displacement front, oil is displaced by the gas phase, which is enclosed by a thin surfactant aqueous film (Heller, 1994; Lee and Heller, 1988). Foam experiments employing a stable displacement front are commonly operated under high-pressure gradients (over 670 kPa/m). SF floods in this study were evaluated under pressure gradients of 20 kPa/m to 200 kPa/m. A stable displacement front was not observed in any of the SF flooding experiments. The fact that no stable displacement front was observed during SF flooding can be explained by comparing the SF mobility with the foam mobilities of the other studies. The

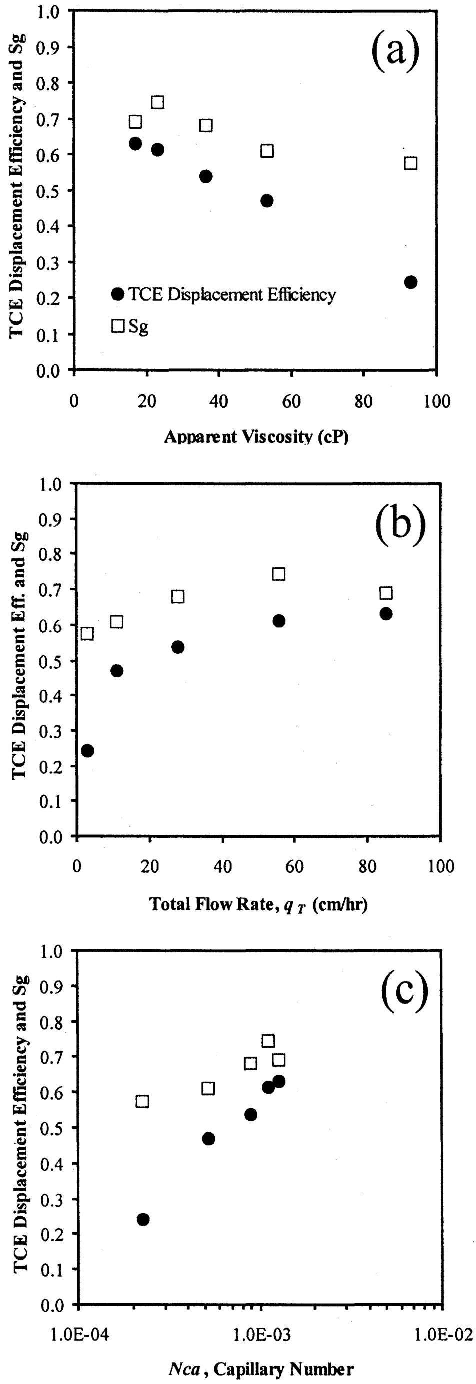

Figure 4. (a) Apparent SF viscosity change with TCE displacement efficiency and gas saturation (S_g); (b) as a function of the total flow rate; and (c) capillary number.

The displacement efficiency was calculated from the ratio of TCE saturation displaced by SF flooding to initial TCE saturation. The GF and the surfactant concentration were 66% and 2%(w), respectively.

two mobilities displayed different ranges. The mobility of foam is usually less than 9.87×10^{-12} cm^2/cp (Heller, 1994; Lee and Heller, 1988; Llave et al., 1990), while the SF mobility of this study ranges from 2×10^{-9} cm^2/cp to 10×10^{-9}

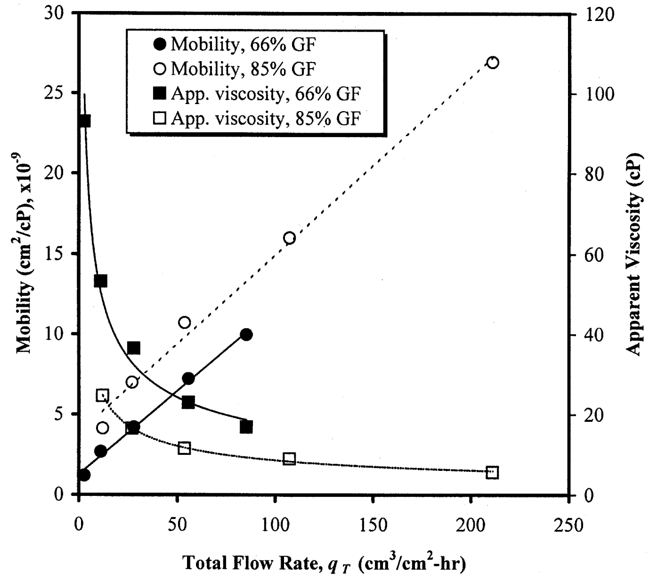

Figure 5. Change in the mobility and apparent viscosity of SF as functions of the total flow rate.

The surfactant concentration was 2% sodium olefin sulfonate(w).

cm^2/cp. The low mobility-foam can propagate with a stable displacement front under higher pressure gradients, while SF under low-pressure gradients may result in flow channeling.

Figure 6 shows the TCE displacement efficiency and gas saturation as a function of SF mobility under the 66% GF condition. The TCE displacement efficiency and gas saturation were nonlinearly proportional to the mobility of SF. As shown in Figure 5, SF demonstrated a decrease in its apparent viscosity and an increase in mobility with an increasing total flow rate. The apparent viscosity decrease implies a decrease in the flow resistance, which would lead to greater spreading of SF, resulting in higher gas saturations. Thus, more residual TCE in the flow channels would also be displaced by the SF flow, leading to higher removal efficiency.

Conclusions

The work presented here demonstrated that the total flow rate of SF and the gas injection velocity were considered to be the most important factors affecting the apparent viscosity and mobility of SF. As the total flow rate of SF and the gas injection velocity (66% GF to 85% GF) increased, the apparent viscosity of SF decreased and the mobility of SF increased. The latter characteristic led to an increase in the TCE displacement efficiency. SF mobility greater than 5×10^{-9} m^2/cp was required to obtain an efficient residual TCE displacement in the homogeneous porous medium that this study used. Thus, the total flow rate and injection velocity of SF can be determined from the SF mobility appropriate for residual TCE removal.

There were some similarities as well as some differences between SF and the other foams in the references. The apparent viscosity and mobility of SF showed trends similar to those of the other foams. However, the results from SF floods and the other foam floods displayed a large difference in the extent of the values of foam properties. The apparent viscos-

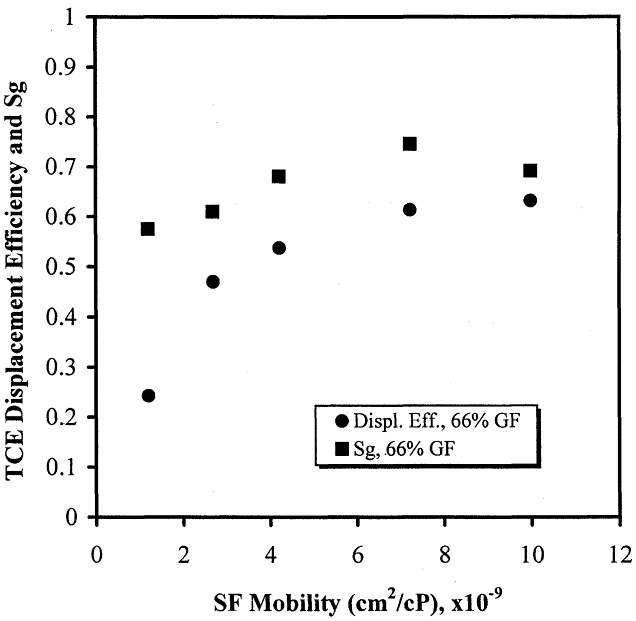

Figure 6. Variation of SF mobility with TCE displacement efficiency and gas saturation (S_g).

The GF and the surfactant concentration were 66% and 2%(w), respectively.

ity of SF was smaller than that of the foam, while the mobility of SF was far larger. The difference can be attributed to the different pressure-gradient range applied.

In SF flooding operated under moderate IFT and pressure gradients, no stable displacement front was observed, and the mobility of foam would be increased, implying flow channeling. However, an increase in the SF mobility resulted in a higher TCE displacement efficiency and gas saturation. Sufficient SF injection velocity causes spreading of foam flow out from the main channels, resulting in the increases in TCE displacement and gas saturation.

Acknowledgment

The authors thank two anonymous reviewers for their constructive comments.

Literature Cited

Buckley, J. S., "Multiphase Displacements in Micromodels," *Interfacial Phenomena in Petroleum Recovery*, Surfactant Sci. Ser., N. R. Morrow, ed., Dekker, New York (1991).

Chang, S.-H., L. Owusu, S. French, and F. Kovarik, "The Effect of Microscopic Heterogeneity on CO_2-Foam Mobility: 2. Mechanistic Foam Simulation," *SPE/DOE Symp. on Enhanced Oil Recovery*, Soc. of Petrol. Eng., (1990).

Chowdiah, P., B. R. Misra, J. J. I. Kilbane, V. J. Srivastava, and T. D. Hayes, "Foam Propagation Through Soils for Enhanced In-Situ Remediation," *J. Hazard. Mat.*, **62**, 265 (1998).

Chu, H., A. Salehzadeh, A. H. Demond, and R. D. Woods, "Mechanisms of Removal of Residual Dodecane Using Surfactant Foam," *NAPLs in Subsurface Environment: Assessment and Remediation Sponsored by the Environmental Engineering* Div., ASCE (1996).

Corey, A. T., *Mechanism of Immiscible Fluids in Porous Media*, Water Resources Publ., CO (1986)

Ettinger, R. A., and C. J. Radke, "Influence of Texture on Steady Foam Flow in Berea Sandstone," *SPE Res. Eng.*, **7**, 83 (1992).

Falls, A. H., J. J. Musters, and R. Ratulowski, "The Apparent Viscosity of Foams in Homogeneous Bead Packs," *SPE Res. Eng.*, **4**, 155 (1989).

Heller, J. P., "CO_2 Foams in Enhanced Oil Recovery," *Foams: Fundamentals and Applications in the Petroleum Industry*, Adv. in Chemistry Ser. 242, L. L. Schramm, ed., ACS (1994).

Hirasaki, G. J., and J. B. Lawson, "Mechanism of Foam Flow in Porous Media: Apparent Viscosity in Smooth Capillaries," *SPE J.*, **25**, 176 (1985).

Hirasaki, G. J., C. A. Miller, R. Szafranski, J. B. Lawson, and N. Akiya, "Surfactant/Foam Process for Aquifer Remediation," *SPE Int. Symp. on Oilfield Chemistry* (1997a).

Hirasaki, G. J., C. A. Miller, R. Szafranski, D. Tanzil, J. B. Lawson, H. Meinardus, M. Jin, J. T. Londergan, R. E. Jackson, G. A. Pope, and W. H. Wade, "Field Demonstration of the Surfactant/Foam Process for Aquifer Remediation," *SPE Technical Conf. and Exhibition*, (1997b).

Hudgins, D. A., and T. H. Chung, "Long-Distance Propagation of Foams, SPE/DOE 20196," *SPE/DOE Symp. on Enhanced Oil Recovery*, (1990).

Huh, D. G., T. D. Cochrane, and F. S. Kovarik, "The Effect of Microscopic Heterogeneity on CO_2 Foam Mobility: 1. Mechanistic study," *J. Pet. Tech.*, **41**, 872 (1989).

Jeong, S.-W., M. Y. Corapcioglu, and S. E. Roosevelt, "Micromodel Study of Surfactant Foam Remediation for Residual Trichloroethylene," *Environ. Sci. Technol.*, **34**, 3456 (2000).

Kovscek, A. R., T. W. Patzek, and C. J. Radke, "Mechanistic Prediction of Foam Displacement in Multidimesions: A Population Balance Approach," SPE/DOE *Symp. on Improved Oil Recovery*, (1994).

Kuhlman, M. I., "Visualizing the Effect of Light Oil on CO_2 Foams," *J. Pet. Tech.*, **42**, 902 (1990).

Lee, H. O., and J. P. Heller, "Carbon Dioxide-Foam Mobility Measurements at High Pressure," *Surfactant-Based Mobility Control*, ACS Symp. Ser., D. H. Smith, ed. (1988).

Lee, H. O., J. P. Heller, and M. W. Hoefer, "Change in Apparent Viscosity of CO_2-Foam with Rock Permeability," *SPE/DOE Symp. on Enhanced Oil Recovery* (1990).

Llave, F. M., F. T. Chung, R. W. Louvier, and D. A. Hudgins, "Foams as Mobility Control Agents for Oil Recovery by Gas Displacement," *SPE/DOE Symp. on Enhanced Oil Recovery* (1990).

Manlowe, D. J., and C. J. Radke, "A Pore-Level Investigation of Foam/Oil Interactions in Porous Media," *SPE Res. Eng.*, **5**, 405 (1990).

Minssiex, L., "Oil Displacement by Foams in Relation to Their Physical Properties in Porous Media," *J. Pet. Tech.*, **26**, 100 (1974).

Owete, O. S. and W. E. Brigham," Flow Behavior of Foam Porous Micromodel Study," *SPE Res. Eng.*, **2**, 315 (1987).

Persoff, P. C., C. J. Radke, K. Pruess, S. M. Benson, and P. A. Witherspoon, "A Laboratory Investigation of Foam Flow in Sandstone at Elevated Pressure," *SPE Res. Eng.*, **6**, 365 (1991).

Ransohoff, T. C., and C. J. Radke, "Mechanism of Foam Generation in Glass-Bead Packs," *SPE Res. Eng.*, **3**, 573 (1988).

Rossen, W. R., Z. H. Zhou, and C. K. Mamun, "Modeling Foam Mobility in Porous Media," *SPE Technical Conf.*, (1991).

Rothmel, R. K., R. W. Peters, E. S. Martin, and M. F. Deflaun, "Surfactant Foam/Bioaugmentation Technology for In Situ Treatment of TCE-DNAPLs," *Environ. Sci. Technol.*, **32**, 1667 (1998).

Stegemeier, G. L. "Mechanisms of Entrapment and Mobilization of Oil in Porous Media." *Improved Oil Recovery by Surfactant and Polymer Flooding*, D. O. Shah and R. S. Schechter, eds., Academic Press, New York (1977).

Schramm, L. L., A. T. Turta, and J. J. Navasad, "Microvisual and Coreflood studies of Foam Interactions with a Light Crude Oil," SPE/DOE Symp. on Enhanced Oil Recovery (1990).

West, C. C., and J. H. Harwell, "Surfactants and Subsurface Remediation," *Environ. Sci. Technol.*, **26**, 2324 (1992).

Manuscript received June 20, 2001, and revision received Aug. 6, 2002.